9-16-2015

Characterization of Line Nanopatterns on Positive Photoresist Produced by Scanning Near-Field Optical Microscope

Sadegh Mehdi Aghaei
Department of Electrical and Computer Engineering, Florida International University, smehdiag@fiu.edu

Navid Yasrebi
Sharif University of Technology

Bizhan Rashidian
Sharif University of Technology

Hindawi Publishing Corporation
Journal of Nanomaterials
Volume 2015, Article ID 936876, 7 pages
http://dx.doi.org/10.1155/2015/936876

Research Article

Characterization of Line Nanopatterns on Positive Photoresist Produced by Scanning Near-Field Optical Microscope

Sadegh Mehdi Aghaei,[1] Navid Yasrebi,[2] and Bizhan Rashidian[2]

[1]*Department of Electrical and Computer Engineering, Florida International University, Miami, FL 33174, USA*
[2]*Department of Electrical Engineering, Sharif University of Technology, Azadi Avenue, Tehran 11155-9363, Iran*

Correspondence should be addressed to Bizhan Rashidian; rashidia@sharif.edu

Received 6 August 2015; Revised 15 September 2015; Accepted 16 September 2015

Academic Editor: Xiaosheng Fang

Line nanopatterns are produced on the positive photoresist by scanning near-field optical microscope (SNOM). A laser diode with a wavelength of 450 nm and a power of 250 mW as the light source and an aluminum coated nanoprobe with a 70 nm aperture at the tip apex have been employed. A neutral density filter has been used to control the exposure power of the photoresist. It is found that the changes induced by light in the photoresist can be detected by *in situ* shear force microscopy (ShFM), before the development of the photoresist. Scanning electron microscope (SEM) images of the developed photoresist have been used to optimize the scanning speed and the power required for exposure, in order to minimize the final line width. It is shown that nanometric lines with a minimum width of 33 nm can be achieved with a scanning speed of 75 μm/s and a laser power of 113 mW. It is also revealed that the overexposure of the photoresist by continuous wave laser generated heat can be prevented by means of proper photoresist selection. In addition, the effects of multiple exposures of nanopatterns on their width and depth are investigated.

1. Introduction

Nanolithography is of particular interest to the semiconductor industry because of shrinking feature sizes as well as increased integration density [1–6]. It is well known that the diffraction limit is one of the challenges faced when reducing dimensions with conventional lithography techniques such as photolithography. Hence, the minimum resolution of patterns created by conventional lithography methods is limited to about $\lambda/2$ [7], where λ is the wavelength of the light. Hence, in order to achieve higher resolutions, expensive optical focalization tools are required.

On the other hand, nanolithography methods based on scanning probe microscopes (SPMs) are good alternatives to the conventional methods because they are able to overcome the Rayleigh limit because of their operation in the near-field. These methods, also known as scanning probe nanolithography (SPL), provide a direct-write method and do not require a separate mask for nanopatterning of the samples. Due to the high cost of masks, especially in very small sizes, and the time-consuming process of their preparation, SPL appears to be economically efficient. Besides, the implementation of SPL is a manageable and executable method in air without the need for vacuum [8]; however, high vacuum tip-enhanced resonance coupling (HV-TERS) system could improve the efficiency of SPMs [9]. Although SPL is a powerful and high resolution nanolithography method, the low speed nature of this process due to pixel by pixel scanning of the sample surface by the probe makes the method unusable for mass production. However, this approach is profitable for fabrication in small quantities [8, 10]. Parallel nanoprobes are used as a way to overcome this constraint, boosting its productivity [11–14]. Atomic force microscope (AFM), scanning tunneling microscope (STM), and scanning near-field optical microscope (SNOM) are among the apparatus which can be modified and used in SPL techniques [15–19]. Patterning with atomic resolution of about 1 Å has been predicted by AFM [1].

Among SPM techniques, the scanning near-field optical nanolithography (SNOL) is a popular one. First outlined by Synge [20], it has been considered as one of the important

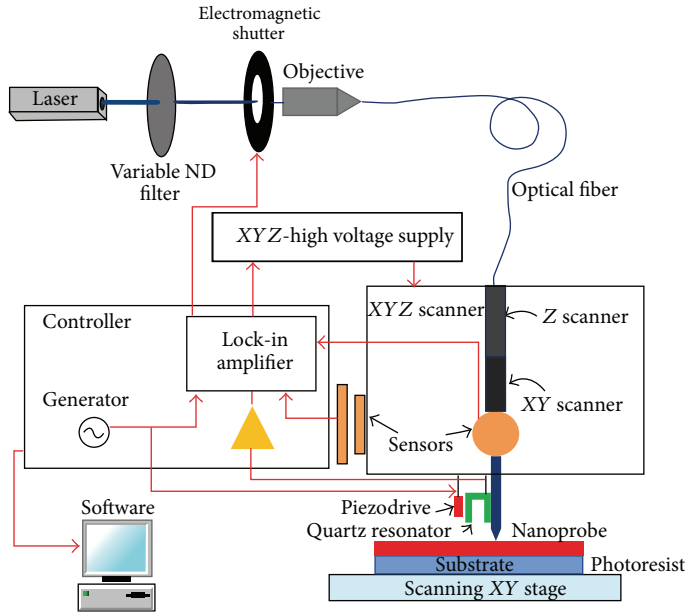

Figure 1: Schematic diagram of the experimental setup for nanopatterning photoresist using SNOM.

nonconventional lithography methods to fabricate nanostructures such as biological nanostructures [21, 22]. The SNOL uses light which leaves no direct effect on the samples and can achieve a resolution significantly higher than $\lambda/2$ so that nanolithography with resolution up to $\lambda/30$ is possible [22]. In SNOL, near-field light generated at the tip of a probe is used as the light source to expose the photoresist. The patterns are implemented with the scanning of the photoresist surface with the tip. SNOL has been successfully demonstrated for patterning of the different materials. Positive photoresist [23, 24], negative photoresist [25], polymethylmethacrylate (PMMA) resists [26, 27], conjugated polymer [28, 29], and azopolymer films [30, 31] are some of organic materials which have been patterned using different lithographic processes. Minimum resolution achieved by this method combined with a femtosecond laser is 20 ± 5 nm with 400 nm light on photoresist [32]. In addition, SNOL has been carried out on inorganic materials such as metals [33–35], H-passivated Si [36], and liquid crystals [37].

In the present work, line nanopatterning of photoresist was carried out using SNOM. A laser diode with a wavelength of 450 nm was used as the power source. This research is focused on the impacts of the experiment conditions on characteristics of the nanopatterns. For this purpose, the effects of scan speed of the probe on the width and depth of nanopatterns were investigated in detail. Furthermore, the size variations of nanopatterns caused by repeating the exposure process of the nanopatterns with the aim of silicon wafer patterning were examined. Obtained results are expected to be a useful experimental reference for nanofabrication applications. Shear force microscope (ShFM) and scanning electron microscope (SEM) were used to characterize the patterns.

The rest of the paper is organized as follows. The experimental setup and preparation of the sample are conducted in Section 2. Section 3 contains experimental results, including measuring width and length of nanopatterns. Finally, Section 4 is devoted to the conclusions.

2. Experimental

A schematic diagram of the experimental system is shown in Figure 1. The NT-MDT Ntegra Solaris SNOM was used to perform this experiment. A 450 nm continuous wave laser diode with maximum output power of 250 mW is employed as the light source. The laser radiation is coupled into a single mode optical fiber and the beam is transmitted into a nanoprobe with an aperture radius of 70 nm. Transmission efficiency of the used probe is 4×10^{-5}. The SNOM nanoprobe is an adiabatic fiber taper which is coated by an aluminum layer with a thickness of 100 nm [38]. The skin depth of the aluminum layer is only about 10 nm [39]; hence, the transmission of the laser light through coating layer could be ignored. A U-shaped quartz resonator is used to control the distance between the tip and the sample surface. This distance should be less than the final desired resolution. During the approaching of the nanoprobe to the sample surface, the resonance frequency and the resonance phase of the system consisting of the nanoprobe and quartz resonator change because of the interactions between the tip and the sample in the atomic scale (ShFM). A feedback loop is used to control and keep a constant distance between tip and sample surface during the scanning. The variations in the tip are detected by a lock-in amplifier which drives the scanner along z-axis to keep the magnitude of the interactions constant during scanning.

For the sample preparation, standard RCA cleaning process was performed. For this purpose, n-type ⟨100⟩ silicon wafers were first cleaned in an ultrasonic bath for 30 minutes in order to remove particles which cannot be removed using standard cleaning process. Second, the silicon wafers were placed into a hot Trichloroethylene (TCE) solution (to remove organic residues), acetone (to remove TCE residues), Isopropyl alcohol (IPA) (to remove acetone residues), and deionized (DI) water with a resistance of 18 MΩ (to remove IPA residues), respectively. In the next step, the wafers were placed into a piranha solution ($H_2SO_4 : H_2O_2$ with 3 : 1 ratio) and DI water, respectively. After that, they were soaked in the SC1 solution (DI water : H_2O_2 : NH_4OH with 5 : 1 : 1 ratio at 75°C) and rinsed with DI water. Then, the wafers were rinsed using the SC2 solution (DI water : HCL : H_2O_2 with 5 : 1 : 1 ratio at 75°C) and finally rinsed with DI water and blow-dried with high purity nitrogen gas. After the cleaning step, a thin layer of Shipley 1813 positive photoresist was deposited on the samples using two stages spin coating. The final thickness is approximately 1.2 μm. To reduce the final photoresist layer thickness, the photoresist has been mixed with the diluent Shipley 1813 before spin coating. In order to increase hardness and adhesion, wafer was baked for 15 min at 90°C in the oven.

The required exposure dose for Shipley 1813 photoresist is approximately 150 mJ/cm^2. It should be noted that chemical absorption at wavelengths less than 400 nm (in the ultraviolet range) is quite remarkable based on the datasheet. Hence, in order to avoid overexposure, some sort of attenuation technique is required. The laser beam power can be attenuated by using a neutral density filter at the laser output, or by means of a conical aperture with low transmission coefficient. The relationship between energy per unit area and output power of the photoresist is given by

$$E = \left(\frac{P_{\text{out}}}{A}\right) \times t, \tag{1}$$

where P_{out} is the power of the light beam at the tip output (laser power multiplied by the filter's transmission coefficient and the probe's transfer efficiency), A is exposure area (equal to the probe's aperture area), and t is exposure time (the average exposure time of the photoresist during aperture movement). If D is assumed as the aperture size, (1) is transformed into the following:

$$E = \left[\frac{\left(P_{\text{in}} \times T_{\text{filter}} \times T_{\text{probe}}\right)}{\left(\pi \times (D/2)^2\right)}\right] \times \left[\frac{D}{v}\right], \tag{2}$$

where v is the scan speed of the tip. Considering transfer efficiency of 4×10^{-5}, an aperture radius of 70 nm, and assuming a scan speed of 10 μm/s, the transfer coefficient of the filter should be approximately 10^{-4}. Therefore, the laser power should be weakened by 10^{-4} times. This can be achieved by adjusting the neutral density filter.

Line nanopatterning of the photoresist was performed by moving the nanoprobe over the sample surface while irradiating the surface by means of the laser beam coupled into the probe. An electromagnetic shutter controlled by specially designed controller (synced to the probe movement) was employed for turning laser light on and off during lithography process. Therefore, the desired pattern could be transferred to the sample. In some cases, *in situ* ShFM was performed in order to monitor the morphology changes on the resist surface after the exposure. The photochemical reactions between near-field light and photoresist make morphologic changes in the resist leading to an altered volume of exposure area and height of resist layer [40]. The resulting changes can be detected due to the sensitivity of the shear force technique to variations of the sample height. Afterward, the samples were dipped in the Shipley 354 solvent solution for 45 seconds and rinsed using DI water for 1 minute and nitrogen-dried. After the development stage, the width and depth of the produced patterns were measured using a SEM.

3. Results and Discussions

Laser beam power at the tip and the scanning speed of the probe are of great importance in SNOL. Since SNOL is based on photochemical reactions in the photoresist layer created by the near-field light, the effective parameter in the width and the depth of patterns is the total energy absorbed by the resist. The higher the energy entered into the photoresist, the higher the volume of the photochemical reactions in the substance, and thereby deeper and wider patterns will be produced. To reduce the pattern size, a low power laser beam with high scanning speed is required to minimize the amount of the light received by the photoresist. Furthermore, in order to avoid melting the metal coating of the SNOM tip, a lower power is recommended. Due to the difficulties in the measurement of the power of near-field light, the scan speed of the tip on the photoresist layer had to be changed for a constant laser power. The distance between the tip and the sample is also important to achieve small feature size. The photoresist will be affected by the evanescent wave emitted from the aperture of the SNOM tip, only if the distance is in the near-field region. Otherwise, the lithography resolution would be limited to the diffraction limit. According to the Bethe-Bouwkamp model [41, 42], the evanescent field has a Gaussian profile. At a specific distance of the tip and the surface, the peak of the laser energy might be higher than the exposure threshold of the photoresist that can expose the photoresist. At this distance, the spot of the peak evanescent energy should be controlled and made smaller than the aperture size [32]. As mentioned before, a feedback loop is employed to control this distance.

Figure 2 shows the one-dimensional (1D) topographic image, 3-dimensional (3D) version of ShFM image (Figure 2(a)), and cross-sectional profile along a line with a length of 25.03 μm (Figure 2(b)) at a scan speed of 10 μm/s. As one can see, the depth of the line is approximately 15 nm and the pattern width (which has been obtained based on the full width at half maximum height (FWHM)) is approximately 200 nm. It should be noted that, for measuring topographical changes of photoresist using ShFM, the patterns were first created in the desired direction by moving the tip over the sample surface and then the sample surface was scanned in the opposite direction by the same tip.

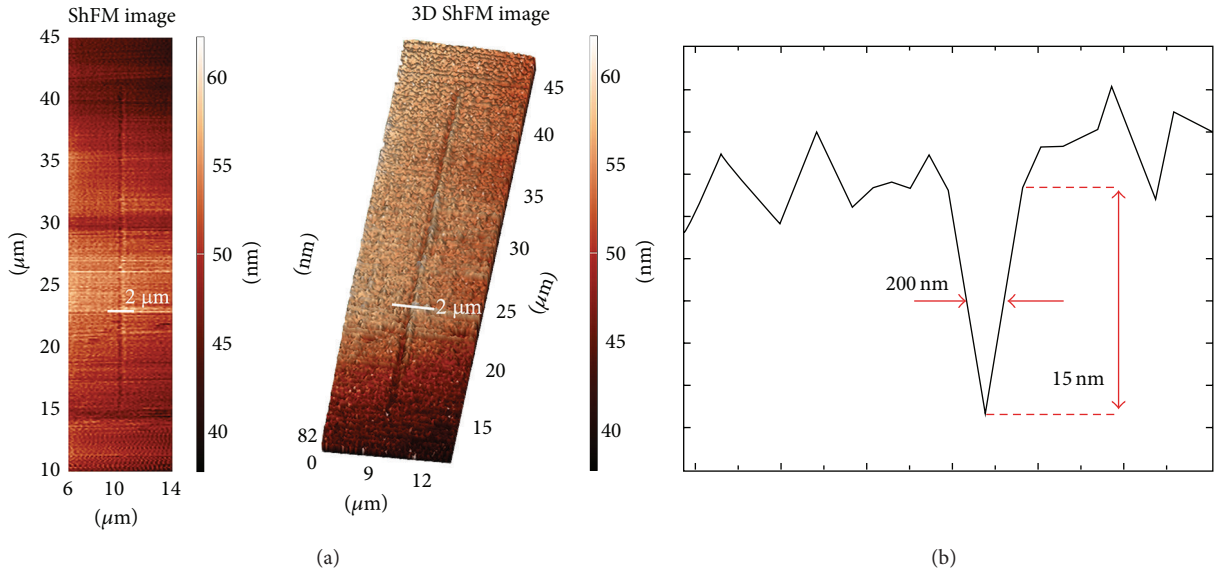

Figure 2: (a) A ShFM image and a 3D version of ShFM image of a line produced by SNOM with scan speed of 10 μm/s at a constant laser power. The shear force feedback is used to detect the morphological changes of the photoresist surface after exposure. (b) Cross-sectional profile of the same line. The measured width and depth of the line are 200 nm and 15 nm, respectively.

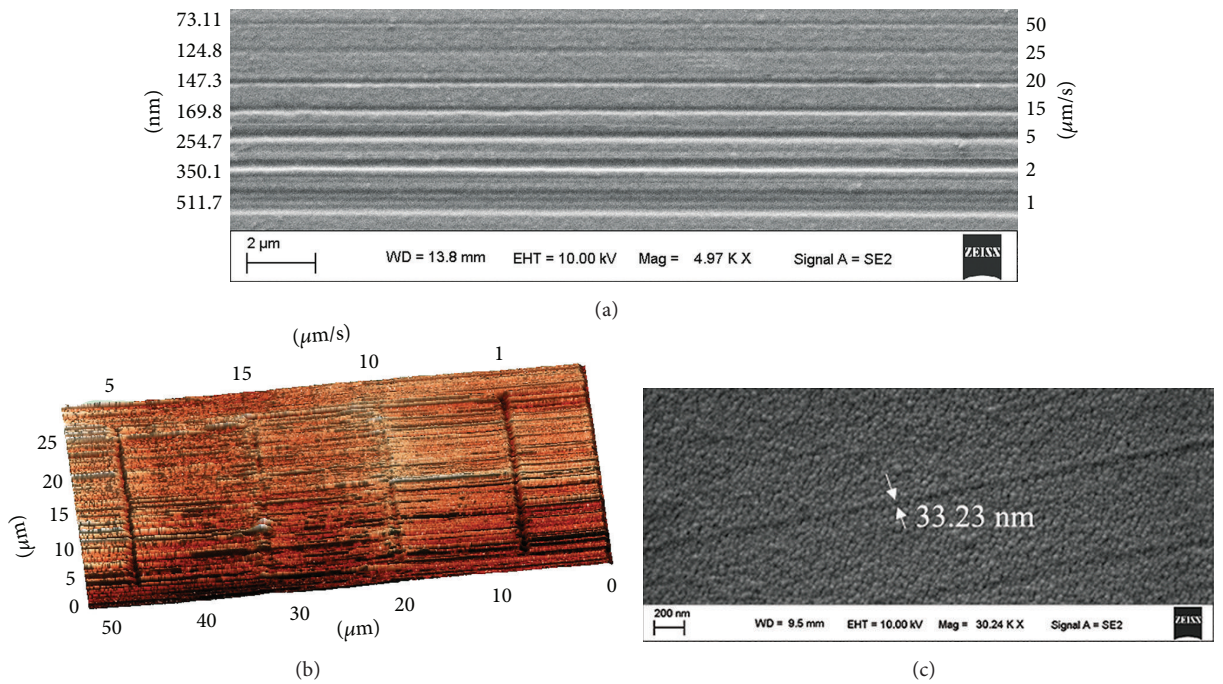

Figure 3: (a) SEM image of the line nanopatterns created with the tip of SNOM at scan speeds of 1, 2, 5, 15, 25, and 50 μm/s. The lines were detected in the developed photoresist samples. (b) The lines revealed through ShFM imaging in the irradiated photoresist before development. The average scan speeds of the tip were set at 1, 5, 10, and 15 μm/s. (c) SEM image of the developed photoresist sample. The best achieved resolution in this experiment produced at scan speed of 75 μm/s. The average thickness of the line is 33.23 nm.

In order to determine the minimum achievable width, the scan speed was increased while keeping the laser power constant. Figure 3(a) shows the SEM image of the line patterns created on the photoresist layer after photoresist development with scanning speeds of 1 μm/s, 2 μm/s, 5 μm/s, 15 μm/s, 20 μm/s, 25 μm/s, and 50 μm/s. The obtained line widths (as measured with the SEM) are 511.7 nm, 350.1 nm, 245.7 nm, 169.8 nm, 147.3 nm, 124.8 nm, and 73.11 nm, respectively. It should be noted that, due to the deposition of a 5–10 nm thick gold layer prior to SEM imaging, the SEM underestimated the value of width and depth of nanopatterns in this case for approximately the same amount. To consolidate the obtained results, topographic predevelopment ShFM images of the patterns with scan speed of 1 μm/s, 5 μm/s, 10 μm/s, and 15 μm/s

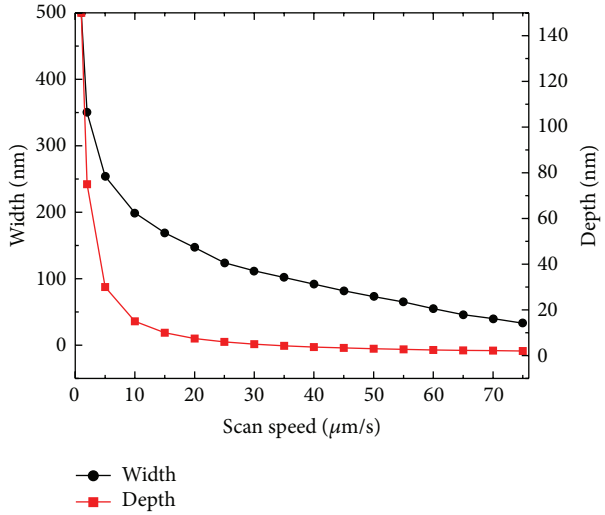

FIGURE 4: Variations of width and depth of line patterns in terms of increasing scan speed of the tip of SNOM at a constant laser power after photoresist development.

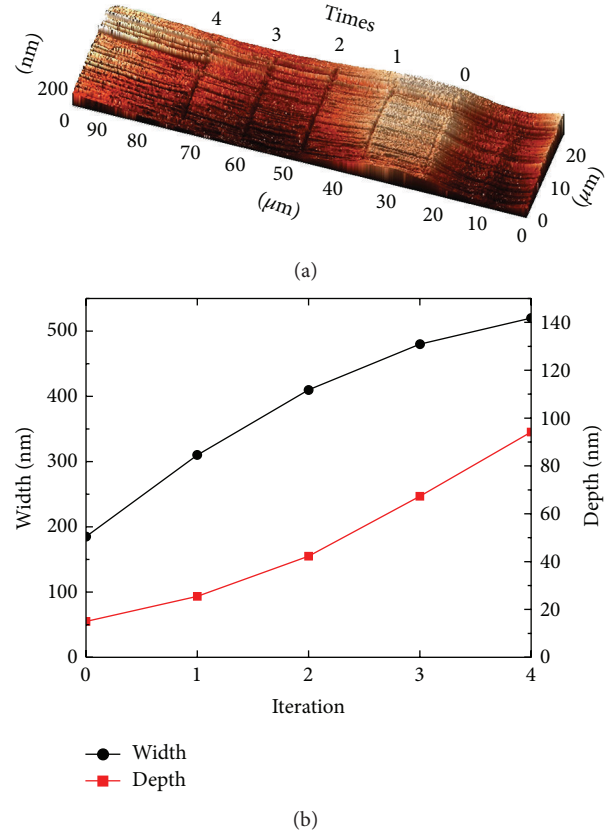

FIGURE 5: (a) 3D version of ShFM image of the line nanopatterns with different number of pattern exposures. The numbers of iterations change from 0 to 4. "0 times" means that the line was produced at a constant laser power with scan speed of 10 μm/s. Topographical changes of the photoresist surface were detected before development stage. (b) Plots of the average width and depth of patterns in terms of the number of iterations of pattern exposure before development of photoresist.

are also presented in Figure 3(b). Our observations show that higher scan speeds make the ShFM observation of the morphological changes more difficult. Finally, as can be seen in Figure 3(c), with a steady increase of scan speed, the minimum visible line width of 33.23 nm (a resolution of about 1/13 of the laser wavelength) was obtained at a scan speed of 75 μm/s. The obtained results are mainly ascribed to the fact that when the tip performs nanolithography with lower scan speeds, it alters the higher volume of the photoresist irradiated areas. But at higher speeds, it only makes superficial scratches on the resist layer without significant altering of resist volume due to less light exposure. Extremely low scan speeds (lower than 5 μm/s) dramatically increase the pattern width and degrade the resolution. This is mainly a result of the Gaussian pattern of the laser output. In other words, while the scanning tip passes through a point on the surface, all adjacent points which are placed in distances below the output spot size (measured as FWHM of the Gaussian beam) are also exposed. Hence, low scanning speed results in multiple exposures of some unwanted points during the exposure process, resulting in extremely low resolution patterns. Figure 4 shows the changes in the pattern width and depth in terms of the scanning speed at constant laser power. As can be seen, pattern width and depth decrease with increasing scan speed; however, depth decreases faster. The energy dose absorbed by the surface of the resist is 20 times larger than that of the resist under the surface [28]. Therefore, the width of the nanopatterns increases faster than the depth at a lower scan speed (higher energy dose).

Theoretically, the photoresist is only polymerized in the illuminated region during the process. However, the energy dose will be affected by the heat of the light due to the pulse duration of the laser. Therefore, a larger area of the photoresist is exposed and that will result in larger patterns. One of the solutions could be using a femtosecond laser to decrease the amount of energy transferred to other regions [32]. As mentioned before, the Shipley 1813 photoresist is an UV photoresist. In this experiment, we employed SNOM combined with a conventional laser, a 450 nm (blue light) continuous wave laser diode, to form nanopatterns on the photoresist. The obtained minimum feature size is dramatically less than the reported results in the similar studies (80–90 nm) when SNOM was combined with conventional laser [23, 24]. It confirms that the heat effects due to the laser pulse duration can be compensated by combining the use of conventional lasers with low sensitivity photoresists.

In order to investigate the effects of radiation on the depth, some of the samples were exposed repeatedly by multiple scanning. Figure 5(a) shows the variations in the width and depth of the patterns with 1–4 times repetitions of the exposure process at 10 μm/s. For the purpose of comparison, one line pattern without multiple exposures is also presented and indicated as "0 time." It is clear that, by increasing the number of exposure iterations, the width and depth of the patterns tend to increase quite significantly, such that, with an increase in iterations from zero to four times, the average depth of the lines increases from 15 nm to 94.2 nm and

the width of lines increases from 195 nm to 520 nm. Therefore, although the final resolution degrades, the aspect ratio (defined by the depth of the patterns divided by the width) increases by a factor of 2 using this approach. This may also maintain the order of magnitude of the lateral dimensions below the wavelength of the laser light. As a result, the produced nanopatterns on photoresist can be transferred to its substrate by reducing the thickness of the photoresist.

4. Conclusion

The potential of SNOL as a powerful method to perform nanolithography was investigated. Line nanopatterns were created by scanning a conical nanoprobe (guiding a 450 nm laser beam) with a 70 nm aperture over the positive photoresist layer. The effect of the scanning speed and multiple exposures of patterns on the width and the depth of the patterns were studied. It was shown that a line width as low as 33 nm (less than 1/13 of the laser wavelength) can be obtained at a scan speed of 75 μm/s, by means of a photoresist with low sensitivity at the laser frequency (here, Shipley 1813), even without femtosecond pulsed-laser beams. It is also found that an increase in the scanning speed results in a direct increasing in lithography resolution. It is also demonstrated that ShFM can be used as a powerful tool for predevelopment characterization of the patterns. Multiple exposures of the samples were performed. The results indicate that although the overall resolution of the lithography process decreases by multiple exposures, the aspect ratio of the pattern increases. This suggests that by proper selection of the experimental conditions (such as resist thickness) high aspect ratio nanopatterns can be produced.

Conflict of Interests

The authors declare that there is no conflict of interests regarding the publication of this paper.

References

[1] S. Landis, *Nano Lithography*, John Wiley Sons, Hoboken, NJ, USA, 2013.

[2] S. Rasappa, L. Schulte, D. Borah, M. A. Morris, and S. Ndoni, "Sub-15 nm silicon lines fabrication via PS-*b*-PDMS block copolymer lithography," *Journal of Nanomaterials*, vol. 2013, Article ID 831274, 7 pages, 2013.

[3] P. Colson, C. Henrist, and R. Cloots, "Nanosphere lithography: a powerful method for the controlled manufacturing of nanomaterials," *Journal of Nanomaterials*, vol. 2013, Article ID 948510, 19 pages, 2013.

[4] X. M. Yang, S. Xiao, Y. Hsu, M. Feldbaum, K. Lee, and D. Kuo, "Directed self-assembly of block copolymer for bit patterned media with areal density of 1.5 Teradot/Inch2 and beyond," *Journal of Nanomaterials*, vol. 2013, Article ID 615896, 17 pages, 2013.

[5] U. K. Thakur, B. G. Kim, S. J. Park, H. W. Baac, D. Lee, and H. J. Park, "Soft-contact printing of nanoparticle-based nanoink for functional nanopatterns," *Journal of Nanomaterials*, vol. 2015, Article ID 723256, 6 pages, 2015.

[6] L. Peng, L. Hu, and X. Fang, "Low-dimensional nanostructure ultraviolet photodetectors," *Advanced Materials*, vol. 25, no. 37, pp. 5321–5328, 2013.

[7] S. Wegscheider, A. Kirsch, J. Mlynek, and G. Krausch, "Scanning near-field optical lithography," *Thin Solid Films*, vol. 264, no. 2, pp. 264–267, 1995.

[8] S. Kwon, W. Chang, and S. Jeong, "Shape and size variations during nanopatterning of photoresist using near-field scanning optical microscope," *Ultramicroscopy*, vol. 105, no. 1–4, pp. 316–323, 2005.

[9] M. Sun, Z. Zhang, L. Chen, and H. Xu, "Tip-enhanced resonance couplings revealed by high vacuum tip-enhanced Raman spectroscopy," *Advanced Optical Materials*, vol. 1, no. 6, pp. 449–455, 2013.

[10] Y. N. Xia, J. A. Rogers, K. E. Paul, and G. M. Whitesides, "Unconventional methods for fabricating and patterning nanostructures," *Chemical Reviews*, vol. 99, no. 7, pp. 1823–1848, 1999.

[11] W. P. King, T. W. Kenny, K. E. Goodson et al., "Atomic force microscope cantilevers for combined thermomechanical data writing and reading," *Applied Physics Letters*, vol. 78, no. 9, pp. 1300–1302, 2001.

[12] P. Vettiger, G. Cross, M. Despont et al., "The 'millipede'—nanotechnology entering data storage," *IEEE Transactions on Nanotechnology*, vol. 1, no. 1, pp. 39–55, 2002.

[13] Z. Liu, E. Ul-Haq, J. K. Hobbs et al., "Parallel scanning near-field photolithography in liquid: the Snomipede," *Microelectronic Engineering*, vol. 88, no. 8, pp. 2109–2112, 2011.

[14] E. U. Haq, Z. Liu, Y. Zhang et al., "Parallel scanning near-field photolithography: the snomipede," *Nano Letters*, vol. 10, no. 11, pp. 4375–4380, 2010.

[15] S. Miyake, M. Wang, and J. Kim, "Silicon nanofabrication by atomic force microscopy-based mechanical processing," *Journal of Nanotechnology*, vol. 2014, Article ID 102404, 19 pages, 2014.

[16] R. D. Piner, J. Zhu, F. Xu, S. Hong, and C. A. Mirkin, "'Dip-pen' nanolithography," *Science*, vol. 283, no. 5402, pp. 661–663, 1999.

[17] S.-W. Hla, K.-F. Braun, and K.-H. Rieder, "Single-atom manipulation mechanisms during a quantum corral construction," *Physical Review B—Condensed Matter and Materials Physics*, vol. 67, no. 20, Article ID 201402, 2003.

[18] A. Houel, D. Tonneau, N. Bonnail, H. Dallaporta, and V. I. Safarov, "Direct patterning of nanostructures by field-induced deposition from a scanning tunneling microscope tip," *Journal of Vacuum Science & Technology B*, vol. 20, no. 6, pp. 2337–2345, 2002.

[19] S. Madsen, S. I. Bozhevolnyi, K. Birkelund, M. Müllenborn, J. M. Hvam, and F. Grey, "Oxidation of hydrogen-passivated silicon surfaces by scanning near-field optical lithography using uncoated and aluminum-coated fiber probes," *Journal of Applied Physics*, vol. 82, no. 1, pp. 49–53, 1997.

[20] E. Synge, "A suggested method for extending microscopic resolution into the ultra-microscopic region," *Philosophical Magazine*, vol. 6, no. 35, pp. 356–362, 2009.

[21] S. Sun, M. Montague, K. Critchley et al., "Fabrication of biological nanostructures by scanning near-field photolithography of chloromethylphenylsiloxane monolayers," *Nano Letters*, vol. 6, no. 1, pp. 29–33, 2006.

[22] M. Montague, R. E. Ducker, K. S. L. Chong et al., "Fabrication of biomolecular nanostructures by scanning near-field photolithography of oligo(ethylene glycol)-terminated self-assembled monolayers," *Langmuir*, vol. 23, no. 13, pp. 7328–7337, 2007.

[23] G. Krausch, S. Wegscheider, A. Kirsch, H. Bielefeldt, J. C. Meiners, and J. Mlynek, "Near field microscopy and lithography with uncoated fiber tips: a comparison," *Optics Communications*, vol. 119, no. 3-4, pp. 283–288, 1995.

[24] A. Naber, H. Kock, and H. Fuchs, "High-resolution lithography with near-field optical microscopy," *Scanning*, vol. 18, no. 8, pp. 567–571, 1996.

[25] X. Yin, N. Fang, X. Zhang, I. B. Martini, and B. J. Schwartz, "Near-field two-photon nanolithography using an apertureless optical probe," *Applied Physics Letters*, vol. 81, no. 19, pp. 3663–3665, 2002.

[26] F. H'dhili, R. Bachelot, G. Lerondel, D. Barchiesi, and P. Royer, "Near-field optics: direct observation of the field enhancement below an apertureless probe using a photosensitive polymer," *Applied Physics Letters*, vol. 79, no. 24, pp. 4019–4021, 2001.

[27] G. Wurtz, R. Bachelot, F. H'Dhili, P. R. C. Triger, C. Ecoffet, and D.-J. Lougnot, "Photopolymerization induced by optical field enhancement in the vicinity of a conducting tip under laser illumination," *Japanese Journal of Applied Physics*, vol. 39, no. 2, pp. L98–L100, 2000.

[28] R. Riehn, A. Charas, J. Morgado, and F. Cacialli, "Near-field optical lithography of a conjugated polymer," *Applied Physics Letters*, vol. 82, no. 4, pp. 526–528, 2003.

[29] D. Credgington, O. Fenwick, A. Charas, J. Morgado, K. Suhling, and F. Cacialli, "High-resolution scanning near-field optical lithography of conjugated polymers," *Advanced Functional Materials*, vol. 20, no. 17, pp. 2842–2847, 2010.

[30] W. Mori, M. Tawata, H. Shimoyama, T. Ikawa, M. Tsuchimori, and O. Watanabe, "Nano-fabrication of azopolymer by scanning near-field optical microscope," *Electronics and Communications in Japan (Part II: Electronics)*, vol. 87, no. 3, pp. 55–61, 2004.

[31] N. Landraud, J. Peretti, F. Chaput et al., "Near-field optical patterning on azo-hybrid sol-gel films," *Applied Physics Letters*, vol. 79, no. 27, pp. 4562–4564, 2001.

[32] Y. Lin, M. H. Hong, W. J. Wang, Y. Z. Law, and T. C. Chong, "Sub-30 nm lithography with near-field scanning optical microscope combined with femtosecond laser," *Applied Physics A*, vol. 80, no. 3, pp. 461–465, 2005.

[33] K. Lieberman, Y. Shani, I. Melnik, S. Yoffe, and Y. Sharon, "Near-field optical photomask repair with a femtosecond laser," *Journal of Microscopy*, vol. 194, no. 2-3, pp. 537–541, 1999.

[34] D. Haefliger and A. Stemmer, "Writing subwavelength-sized structures into aluminium films by thermo-chemical apertureless near-field optical microscopy," *Ultramicroscopy*, vol. 100, no. 3-4, pp. 457–464, 2004.

[35] S. Nolte, B. N. Chichkov, H. Welling, Y. Shani, K. Lieberman, and H. Terkel, "Nanostructuring with spatially localized femtosecond laser pulses," *Optics Letters*, vol. 24, no. 13, pp. 914–916, 1999.

[36] M. K. Herndon, R. T. Collins, R. E. Hollingsworth, P. R. Larson, and M. B. Johnson, "Near-field scanning optical nanolithography using amorphous silicon photoresists," *Applied Physics Letters*, vol. 74, no. 1, pp. 141–143, 1999.

[37] P. J. Moyer, K. Walzer, and M. Hietschold, "Modification of the optical properties of liquid crystals using near−field scanning optical microscopy," *Applied Physics Letters*, vol. 67, no. 15, pp. 2129–2131, 1995.

[38] E. Betzig, J. K. Trautman, T. D. Harris, J. S. Weiner, and R. L. Kostelak, "Breaking the diffraction barrier: optical microscopy on a nanometric scale," *Science*, vol. 251, no. 5000, pp. 1468–1470, 1991.

[39] M. A. Paesler and P. J. Moyer, *Near-Field Optics, Theory, Instrumentation, and Applications*, vol. 68, Wiley, New York, NY, USA, 1st edition, 1996.

[40] C. C. Davis, W. A. Atia, A. Güngör, D. L. Mazzoni, S. Pilevar, and I. I. Smolyaninov, "Scanning near-field optical microscopy and lithography with bare tapered optical fibers," *Laser Physics*, vol. 7, no. 1, pp. 243–256, 1997.

[41] H. A. Bethe, "Theory of diffraction by small holes," *Physical Review*, vol. 66, no. 7-8, pp. 163–170, 1944.

[42] C. J. Bouwkamp, "Diffraction theory," *Reports on Progress in Physics*, vol. 17, no. 1, pp. 35–100, 1954.